J. Am. Chem. Soc. 1990, 112, 7900–7903

Gas-Phase Inorganic Chemistry: Laser Spectroscopy of Calcium and Strontium Monoborohydrides

F. S. Pianalto,[†] **A. M. R. P. Bopegedera,**[‡] **W. T. M. L. Fernando, R. Hailey, L. C. O'Brien,**[§] **C. R. Brazier,**[⊥] **P. C. Keller, and P. F. Bernath**[*,‖]

Contribution from the Department of Chemistry, The University of Arizona, Tucson, Arizona 85721. *Received April 13, 1990*

Abstract: The $CaBH_4$ and $SrBH_4$ free radicals were synthesized by the reaction of Ca or Sr vapor with diborane, B_2H_6. The $\tilde{A}^2A_1$–$\tilde{X}^2A_1$ and $\tilde{B}^2E$–$\tilde{X}^2A_1$ electronic transitions were detected by laser-induced fluorescence. The spectra are consistent with tridentate molecular structures with three bridging hydrogens and C_{3v} symmetry.

Introduction

The tetrahydroborate anion (BH_4^-) forms a large number of interesting ionic and covalent complexes with metals.[1,2] The coordination between the metal and the BH_4^- ion invariably occurs through bridging hydrogens, and rapid interconversion between the various coordination modes is known in the liquid phase.[1,2]

BH_4^- is a commonly used reducing agent. Nevertheless, very little is known about the spectroscopic properties of the metal–BH_4 complexes, particularly in the gas phase. Of the alkaline earth borohydrides, only $Be(BH_4)_2$ has been analyzed in the gas phase, but the molecular structure remains uncertain. Gundersen, Hedberg, and Hedberg[3] studied the $Be(BH_4)_2$ structure using electron diffraction methods, while Nibler[4] examined the infrared and Raman spectra. The gas-phase NMR spectrum shows only a single set of equivalent protons, consistent with fluxional behavior.[5] A recent theoretical calculation by Stanton, Lipscomb, and Bartlett[6] has provided new insight into this long-standing problem.

In contrast to the covalent $Be(BH_4)_2$, the alkali borohydrides and the heavier alkaline earth borohydrides are all ionic solids with low vapor pressures.[1,2] We report here on the discovery of the gas-phase calcium and strontium monoborohydride free radicals, $CaBH_4$ and $SrBH_4$. These molecules are made by the reaction of Ca and Sr vapors with diborane, B_2H_6. The observation of $CaBH_4$ completes the isoelectronic p-block family of molecules, $CaBH_4$, $CaCH_3$,[7] $CaNH_2$,[8] CaOH,[9] and CaF.[10] We have previously studied many monovalent derivatives of Ca and Sr in our laboratory, including carboxylates,[11] azides,[12] isocyanates,[13] cyclopentadienides,[14] acetylides,[15] formamidates,[16] pyrrolates,[17] alkanamides,[18] and alkoxides.[19]

$CaBH_4$ and $SrBH_4$ are the first examples of gas-phase metal monoborohydrides to be experimentally characterized. However, there has been considerable theoretical activity in this area. Ab initio predictions for the properties of $LiBH_4$,[20-25] $NaBH_4$,[23-26] KBH_4[24] and $CuBH_4$[24] are available in the literature. The structures are all predicted to be fluxional with either tridentate or bidentate (for $CuBH_4$) coordination. There is the tantalizing possibility of observing some evidence of fluxional behavior in the spectra of $CaBH_4$ and $SrBH_4$.

Experimental Methods

The calcium and strontium borohydrides were produced in a Broida oven[27] by the reaction of Ca or Sr with diborane (B_2H_6), similar to previous work[7-19] in this area. The Ca or Sr metal was vaporized from a resistively heated crucible, carried to the reaction region by argon carrier gas, and reacted with diborane. The diborane was stored as a solid in a liquid nitrogen bath. During the experiment, the diborane was melted with a pentane/liquid N_2 bath (−130 °C) and added as a gas to the Broida oven. The pressures were approximately 1 Torr of argon and 0.035 Torr of diborane.

The diborane was prepared by slowly adding sodium borohydride ($NaBH_4$) to heated polyphosphoric acid under vacuum. The diborane gas produced was collected with a liquid N_2 bath.

Two types of low-resolution spectra were recorded. Laser excitation spectra were obtained by scanning a broad-band (1 cm^{-1}) CW dye laser through a spectral region where $CaBH_4$ or $SrBH_4$ absorb and detecting total fluorescence through red pass filters with a photomultiplier tube. Resolved fluorescence spectra were obtained by fixing the dye laser at

---

[†] Current Address: U.S.D.A., Western Human Nutrition Research Center, Post Office Box 29997, Presidio of San Francisco, CA 94129.

[‡] Current Address: NOAA, ERL, R/E/AL2, 325 Broadway, Boulder, CO 80303.

[§] Current Address: Department of Chemistry Southern Illinois University at Edwardsville, Edwardsville, IL 62026.

[⊥] Current Address: Astronautics Lab./LSX, Edwards AFB, CA 93523.

[‖] Alfred P. Sloan Fellow; Camille and Henry Dreyfus Teacher-Scholar.

(1) James, B. D.; Wallbridge, M. G. H. *Prog. Inorg. Chem.* **1970**, *11*, 99–231.

(2) Marks, T. J.; Kolb, J. R. *Chem. Rev.* **1977**, *77*, 263–293.

(3) Gundersen, G.; Hedberg, L.; Hedberg, K. *J. Chem. Phys.* **1973**, *59*, 3777–3785.

(4) Nibler, J. W. *J. Am. Chem. Soc.* **1972**, *94*, 3349–3359.

(5) Gaines, D. F.; Walsh, J. L.; Morris, J. H.; Hillenbrand, D. F. *Inorg. Chem.* **1978**, *17*, 1516–1522.

(6) Stanton, J. F.; Lipscomb, W. N.; Bartlett, R. J. *J. Chem. Phys.* **1988**, *88*, 5726–5734.

(7) Brazier, C. R.; Bernath, P. F. *J. Chem. Phys.* **1987**, *86*, 5918–5922; **1989**, *91*, 4548–4554.

(8) Wormsbecher, R. F.; Penn, R. E.; Harris, D. O. *J. Mol. Spectrosc.* **1983**, *97*, 65–72.

(9) Bernath, P.; Kinsey-Nielsen, S. *Chem. Phys. Lett.* **1984**, *105*, 663–666. Bernath, P. F.; Brazier, C. R. *Astrophys. J.* **1985**, *288*, 373–376.

(10) Bernath, P.; Field, R. W. *J. Mol. Spectrosc.* **1980**, *82*, 339–347. Dulick, M.; Bernath, P.; Field, R. W. *Can. J. Phys.* **1980**, *58*, 703–712.

(11) O'Brien, L. C.; Brazier, C. R.; Kinsey-Nielsen, S.; Bernath, P. F. *J. Phys. Chem.* **1990**, *94*, 3543–3547.

(12) Brazier, C. R.; Bernath, P. F. *J. Chem. Phys.* **1988**, *88*, 2112–2116.

(13) Ellingboe, L. C.; Bopegedera, A. M. R. P.; Brazier, C. R.; Bernath, P. F. *Chem. Phys. Lett.* **1986**, *126*, 285–289. O'Brien, L. C.; Bernath, P. F. *J. Chem. Phys.* **1988**, *88*, 2117–2120.

(14) O'Brien, L. C.; Bernath, P. F. *J. Am. Chem. Soc.* **1986**, *108*, 5017–5018.

(15) Bopegedera, A. M. R. P.; Brazier, C. R.; Bernath, P. F. *Chem. Phys. Lett.* **1987**, *136*, 97–100; *J. Mol. Spectrosc.* **1988**, *129*, 268–275.

(16) Bopegedera, A. M. R. P.; Fernando, W. T. M. L.; Bernath, P. F. *J. Phys. Chem.* **1990**, *94*, 3547–3549.

(17) Bopegedera, A. M. R. P.; Fernando, W. T. M. L.; Bernath, P. F. *J. Phys. Chem.* **1990**, *94*, 4476–4479.

(18) Bopegedera, A. M. R. P.; Brazier, C. R.; Bernath, P. F. *J. Phys. Chem.* **1987**, *91*, 2779–2781.

(19) Brazier, C. R.; Ellingboe, L. C.; Kinsey-Nielsen, S.; Bernath, P. F. *J. Am. Chem. Soc.* **1986**, *108*, 2126–2132.

(20) Dill, J. D.; Schleyer, P. v. R.; Binkley, J. S.; Pople, J. A. *J. Am. Chem. Soc.* **1977**, *99*, 6159–6173. DeFrees, D. J.; Raghavachari, K.; Schlegel, H. B.; Pople, J. A.; Schleyer, P. v. R. *J. Phys. Chem.* **1987**, *91*, 1857–1864.

(21) Boldyrev, A. I.; Charkin, O. P.; Rambidi, N. G.; Avdeev, V. I. *Chem. Phys. Lett.* **1976**, *44*, 20–24; *Zhur. Strukt. Khim.* **1977**, *18*, 13–22.

(22) Kello, V.; Urban, M.; Boldyrev, A. I. *Chem. Phys. Lett.* **1984**, *106*, 455–459.

(23) Baranov, L. Ya.; Boldyrev, A. I. *Chem. Phys. Lett.* **1983**, *96*, 218–222.

(24) Charkin, O. P.; Musaev, D. G.; Klimenko, M. N. *Koord. Khim.* **1985**, *11*, 409–414.

(25) Bonaccorsi, R.; Scrocco, E.; Tomasi, J. *Theor. Chim. Acta* **1979**, *52*, 113–127.

(26) Barone, V.; Dolcetti, G.; Lelj, F.; Russo, N. *Inorg. Chem.* **1981**, *20*, 1687–1691.

(27) West, J. B.; Bradford, R. S.; Eversole, J. D.; Jones C. R. *Rev. Sci. Instrum.* **1975**, *46*, 164–168.

0002-7863/90/1512-7900$02.50/0

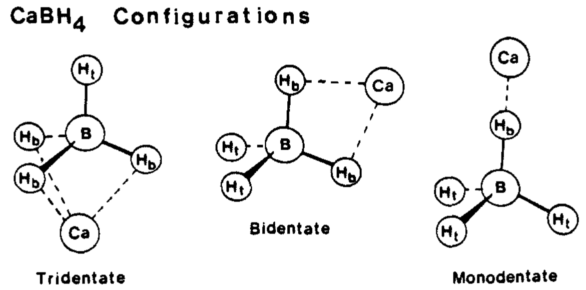

Figure 1. Three possible structures of $CaBH_4$ with Ca^+ bonded to a BH_4^- tetrahedron are likely: tridentate (three bridging hydrogens), bidentate (two bridging hydrogens), and monodentate (one bridging hydrogen). Figure 1 is very similar to the diagram in the work of Boldyrev et al.[20] By analogy with the ionic alkali monoborohydrides, the monodentate structure is expected to lie quite high in energy. The tridentate and bidentate structures should lie close in energy with the tridentate structure the global minimum on the potential surface. If the molecule is fluxional the bidentate structures may be transition states between the four tridentate minima.

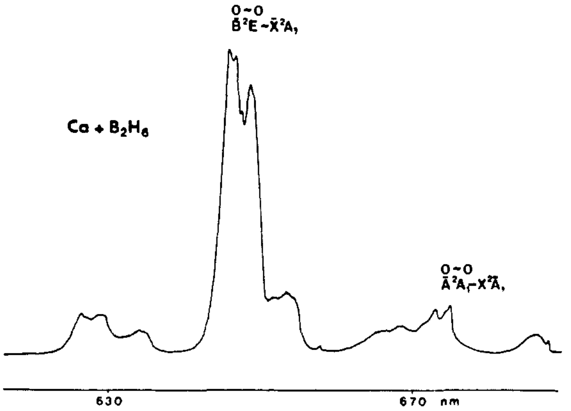

Figure 2. This is the laser excitation spectrum of $CaBH_4$. The 0–0 vibrational bands of the $\tilde{B}^2E-\tilde{X}^2A_1$ and $\tilde{A}^2A_1-\tilde{X}^2A_1$ transitions are labeled. Only the Ca–BH_4 stretching modes have Franck–Condon activity. The relative intensities of the two transitions are distorted by the effects of variation in laser power with frequency and the use of a red-pass filter for detection. The small features at 6550 and 6350 Å are the 1–0 and 2–0 bands of the $\tilde{A}^2A_1-\tilde{X}^2A_1$ transition, and the small features at 6290 and 6675 Å are the 1–0 and 0–1 bands of the $\tilde{B}^2E-\tilde{X}^2A_1$ transition.

the frequency of a $CaBH_4$ or $SrBH_4$ molecular transition and scanning the wavelength of a monochromator to detect laser-induced fluorescence.

In similar Broida oven experiments, a second dye laser tuned to the Ca or Sr $^3P_1-^1S_0$ atomic line was required to promote the reaction between the alkaline earth vapor and the various oxidants. The reaction between Ca or Sr with diborane, however, was vigorous enough to be detected without the use of the second dye laser to excite the metal atom.

Results and Discussion

The spectra of the calcium and strontium borohydrides were assigned by comparison to the spectra of other alkaline earth molecules.[7-19] Transitions to two excited states were observed, and these were assigned $\tilde{A}^2A_1-\tilde{X}^2A_1$, $\tilde{B}^2E_{1/2}-\tilde{X}^2A_1$, and $\tilde{B}^2E_{3/2}-\tilde{X}^2A_1$. The presence of a spin–orbit splitting (and its magnitude) in the ^2E state suggests a symmetric top structure. The structural assignment of C_{3v} symmetry is consistent with the predicted lowest energy tridentate structure (see Figure 1) of the ab initio[20-26] calculations on the ionic $LiBH_4$, $NaBH_4$, and KBH_4 molecules.

Figure 2 is a portion of a $CaBH_4$ laser excitation scan. The 0–0 bands of the $\tilde{A}^2A_1-\tilde{X}^2A_1$ and the $\tilde{B}^2E-\tilde{X}^2A_1$ transitions are labeled. The 1–0 and 2–0 bands of the $\tilde{A}^2A_1-\tilde{X}^2A_1$ transition appear as the small features at approximately 6550 and 6350 Å, respectively. The 1–0 and 0–1 bands of the $\tilde{B}^2E-\tilde{X}^2A_1$ transition appear at approximately 6290 and 6675 Å, respectively. The $^2E_{3/2}$ spin component of the $\tilde{B}^2E$ state at higher energy is slightly more intense than the $^2E_{1/2}$ spin component, and the spin–orbit coupling constant of the $\tilde{B}^2E$ state is approximately 59 cm^{-1} for $CaBH_4$ and 200 cm^{-1} for $SrBH_4$. These values are somewhat lower than what is typically observed for calcium (65–75 cm^{-1}) and strontium (260–290 cm^{-1}) bonding with other ligands (Table III). The low values might be due to the three bridging hydrogens involved in the metal–ligand bond. They could act to diminish the spin–orbit interaction by increasing the amount of d-character in the $\tilde{B}^2E$ state or by Jahn–Teller quenching of the orbital angular momentum about the top axis.

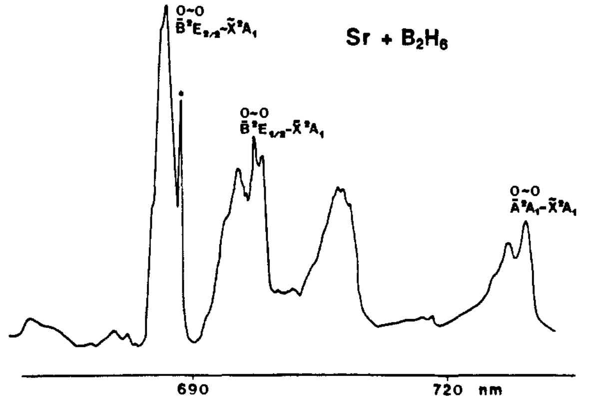

Figure 3. This is a laser excitation spectrum of $SrBH_4$. The 0–0 vibrational bands of the $\tilde{B}^2E-\tilde{X}^2A_1$ and $\tilde{A}^2A_1-\tilde{X}^2A_1$ transitions are labeled. Like $CaBH_4$, only the Sr–BH_4 stretching mode displays Franck–Condon activity. The feature at 7075 Å is a blend of the 1–0 band of the $\tilde{A}^2A_1-\tilde{X}^2A_1$ transition and the 0–1 vibration of the $\tilde{B}^2E-\tilde{X}^2A_1$ transition. The asterisk marks the Sr $^3P_1-^1S_0$ atomic line.

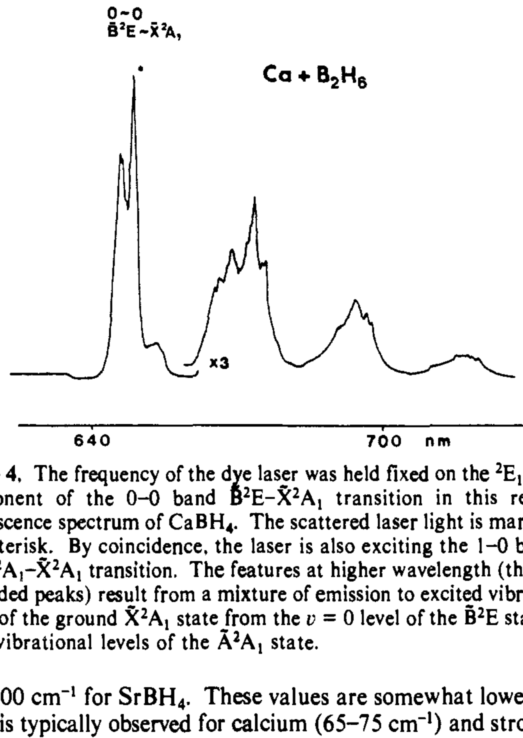

Figure 4. The frequency of the dye laser was held fixed on the $^2E_{1/2}$-spin component of the 0–0 band $\tilde{B}^2E-\tilde{X}^2A_1$ transition in this resolved fluorescence spectrum of $CaBH_4$. The scattered laser light is marked by the asterisk. By coincidence, the laser is also exciting the 1–0 band of the $\tilde{A}^2A_1-\tilde{X}^2A_1$ transition. The features at higher wavelength (the three expanded peaks) result from a mixture of emission to excited vibrational levels of the ground $\tilde{X}^2A_1$ state from the $v = 0$ level of the $\tilde{B}^2E$ state and from vibrational levels of the $\tilde{A}^2A_1$ state.

The laser excitation spectrum of $SrBH_4$ is shown in Figure 3. The 0–0 bands of the $\tilde{B}^2E-\tilde{X}^2A_1$ transitions and the $\tilde{A}^2A_1-\tilde{X}^2A_1$ transition are labeled. The large unlabeled peak is a blend of the $\tilde{B}^2E-\tilde{X}^2A_1$ 0–1 band and the $\tilde{A}^2A_1-\tilde{X}^2A_1$ 1–0 band. The asterisk marks the Sr atomic line at 6892 Å.

A portion of a $CaBH_4$-resolved fluorescence spectrum is shown in Figure 4. To record this spectrum, the dye laser was fixed at the frequency of the $^2E_{1/2}$ spin component of the $\tilde{B}^2E$ state while the monochromator was scanned. By coincidence, the laser is also positioned at the frequency of the 1–0 band of the $\tilde{A}^2A_1-\tilde{X}^2A_1$ transition. The asterisk marks the scattered light from the laser. The blue (higher energy) side of the first expanded feature at approximately 6550 Å consists mostly of fluorescence to the vibrational level $v = 1$ of the $\tilde{X}^2A_1$ state from the $v = 0$ level of the $\tilde{B}^2E_{1/2}$ state (0–1 band). The red (lower energy) side of the feature is mostly due to fluorescence from the $v = 0$ level of the $\tilde{A}^2A_1$ state to the $v = 0$ level of the $\tilde{X}^2A_1$ state (0–0 band at 6750

Table I. Band Origins for the $CaBH_4$ and $SrBH_4$ Vibronic Transitions (cm^{-1})

band	$CaBH_4$	$SrBH_4$
	$\tilde{B}^2E_{3/2}$–$\tilde{X}^2A_1$	
2–0		15347[a]
1–0	15934	14939
0–0	15458	14529
0–1	15006	14134
	$\tilde{B}^2E_{1/2}$–$\tilde{X}^2A_1$	
2–0		15144
1–0	15865	14739
0–0	15394	14331
0–1	14948	13937
	$\tilde{A}^2A_1$–$\tilde{X}^2A_1$	
2–0	15741	
1–0	15272	14127
0–0	14804	13723
0–1	14349	13333
0–2	13895	12953

[a] Errors are approximately ±10 cm^{-1}.

Table II. Vibrational Frequencies for $CaBH_4$ and $SrBH_4$ (cm^{-1})

state	$CaBH_4$	$SrBH_4$
$\tilde{B}^2E$	472[a]	408
$\tilde{A}^2A_1$	469	404
$\tilde{X}^2A_1$	455	388

[a] Errors are approximately ±10 cm^{-1}.

Å). The other two expanded features at approximately 6900 and 7300 Å also result from mixtures of emission to excited vibrational levels of the ground $\tilde{X}^2A_1$ state from the $v = 0$ level of the $\tilde{B}^2E$ state and the $v = 0$ level of the $\tilde{A}^2A_1$ state.

Band origins determined for $CaBH_4$ and $SrBH_4$ are presented in Table I. For each band, the origin was determined by averaging values from both laser excitation and resolved fluorescence scans. Finally, vibrational frequencies for the three observed states were determined from the band origins and are presented in Table II. Because the electronic transitions are centered on the metal atom, only one mode, the M–BH_4 stretch, displays Franck–Condon activity.

Ab initio calculations are not available for $CaBH_4$ or $SrBH_4$, but the predictions[20-26] for $LiBH_4$, $NaBH_4$, and KBH_4 are very helpful. The presence of an extra nonbonding electron in the corresponding alkaline earth monoborohydrides should not greatly affect the geometric structure. In Figure 1, the three most likely structures are shown. The tridentate configuration is best described as Ca^+ bonding to one face of the BH_4^- tetrahedron through three bridging hydrogens. The bidentate structure has the Ca^+ ion bonding to the edge of the BH_4^- tetrahedron with two bridging hydrogens. Finally, the monodentate structure has the Ca^+ bonding to a vertex of the BH_4^- tetrahedron through a single hydrogen atom. The point groups are C_{3v}, C_{2v}, and C_{3v} for the tridentate, bidentate, and monodentate bonding, respectively.

The ab initio calculations[20-26] consistently predict that the monodentate structure lies about 20 kcal/mole higher in energy than the bidentate and tridentate structures. Also, monodentate coordination has never been observed in a metal borohydride,[1,2] so is not likely to be important for $CaBH_4$ or $SrBH_4$.

Our assignment of C_{3v} symmetry for $CaBH_4$ and $SrBH_4$ rests on the similarity between the spectra of these molecules and the spectra of, for example, $CaCH_3$,[5] CaN_3,[12] and CaC_5H_5,[14] which all have axial symmetry (i.e., an axis of rotational symmetry, C_n, with $n > 2$). If the $CaBH_4$ molecule has C_{2v} symmetry with bidentate coordination (Figure 1), then the excited ^2E state would split into two electronic states of $^2B_1$ and $^2B_2$ symmetry similar to $CaNH_2$[8,18] and CaO_2CH.[11] If the $CaBH_4$ molecule has C_{3v} symmetry (Figure 1), then the ^2E state will split into two spin components, $^2E_{1/2}$ and $^2E_{3/2}$, like $CaCH_3$.[7] For comparison purposes, other spin–orbit splittings for the ^2E and $^2\Pi$ states of monovalent alkaline earth derivatives are provided in Table III. On the whole, the $CaBH_4$ and $SrBH_4$ ^2E state splittings are more suggestive of a C_{3v} spin–orbit splitting than a $^2B_1$–$^2B_2$ electronic splitting.

Table III. Observed Spin–Orbit Splittings (cm^{-1}) for the Lowest $^2\Pi$ or ^2E States of Some Alkaline Earth Containing Free Radicals, ML (M = Ca or Sr and L = Ligand)

molecule	CaL	SrL	molecule	CaL	SrL
MF[a]	73	281	MNCO[f]	68	293
MOH[b]	67	264	MCH_3[g]	73	309
$MOCH_3$[c]	65	268	MC_5H_5[h]	57	255
MCCH[d]	70	275	MBH_4[i]	59	200
MN_3[e]	76	296			

[a] References 10 and 29. [b] References 9 and 30. [c] References 19 and 28. [d] Reference 15. [e] Reference 12. [f] Reference 13. [g] Reference 7. [h] Reference 14. [i] This work.

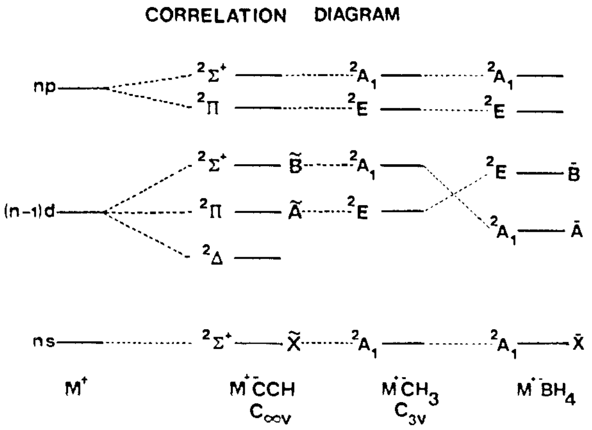

Figure 5. This correlation diagram shows the effects of various ligands perturbing the metal ion (Sr^+ and Ca^+) atomic orbitals. The ordering of the first excited states, ^2E and $^2A_1$, for MBH_4 radicals is reversed when compared with the MCH_3 radicals. The difference in ordering is attributed to differences in ionic bonding. For the MCH_3 molecules, bonding occurs on the metal–ligand axis, between the alkaline earth cation M^+ and the negatively charged carbon. For the MBH_4 molecules, however, bonding also occurs off the metal–ligand axis, between the cation M^+ and three bridging hydrogens that bear a partial negative charge. This partial negative charge destabilizes the off-axis ^2E state relative to the $^2A_1$ state. The atomic orbital character of ^2E and $^2A_1$ states and the nature of the metal–ligand bond determine the relative ordering of the states.

Calcium borohydride is currently being analyzed using high-resolution laser techniques in an attempt to make a definite assignment of the states observed, and to determine the molecular rotational constants. Several sub-bands of the $\tilde{B}^2E$–$\tilde{X}^2A_1$ transition have been recorded but the fits to determine the molecular constants were not very reasonable, presumably because of the perturbations. However, there was no sign of the expected splitting[23] of the rotational lines due to the fluxional behavior of $CaBH_4$. Either the fluxional motion is so fast that very large splittings result or so slow that the small splittings were not resolved.

The expected size of these splittings is hard to predict because they depend critically on the unknown height of the barrier for the BH_4^- internal rotation. For example, Baranov and Boldyrev[23] calculate a ground state splitting of 6×10^{-5} cm^{-1} for $LiBH_4$ if the barrier is about 1000 cm^{-1}, but if the barrier drops to about 600 cm^{-1} (e.g. in $LiCH_4^+$), then the tunnelling splitting is calculated[23] to be 0.001 cm^{-1}. As is often the case for fluxional behavior, the study of deuterated derivatives may also prove to be useful.

The ordering of the excited states of the alkaline earth borohydrides is surprising. Previously analyzed symmetric top molecules ($CaCH_3$,[7] $SrCH_3$[7] and $SrOCH_3$[28]) have ^2E states lower

---

(28) O'Brien, L. C.; Brazier, C. R.; Bernath, P. F. *J. Mol. Spectrosc.* **1988**, *130*, 33–45.

(29) Steimle, T. C.; Domaille, P. J.; Harris, D. O. *J. Mol. Spectrosc.* **1978**, *73*, 441–443. Nakagawa, J.; Domaille, P. J.; Steimle, T. C.; Harris, D. O. *J. Mol. Spectrosc.* **1978**, *70*, 374–385. Field, R. W.; Harris, D. O.; Tanaka, T. *J. Mol. Spectrosc.* **1975**, *57*, 107–117.

in energy than ${}^2A_1$ states, whereas in the borohydrides the ordering is reversed (Figure 5). In this respect the $CaBH_4$ and $SrBH_4$ molecules resemble the formate derivatives,[11] CaO_2CH and SrO_2CH (as well as the formamidate[16] derivatives). The ${}^2A_1$ states of the formates[11] lie lower in energy than the ${}^2B_1$, ${}^2B_2$ pair of states which correlate to the ${}^2E$ or ${}^2\Pi$ states of a high symmetry axial ligand.

The alkaline earth borohydride and formate molecules share one striking similarity. In each one bonding occurs off the metal-ligand axis with bridging ligand atoms (three hydrogens for the borohydrides and two oxygens for the formates). The bridging atoms have a partial negative charge. When they point towards the off-axis Ca^+ and Sr^+ p- and d-orbitals containing the excited electron, the π-like orbitals are destabilized relative to the on-axis σ-like orbitals.

In the cases of the methyl and methoxy derivatives, bonding occurs on the metal-ligand axis so the negative charge of the ligand points to the on-axis orbitals of the cation. When containing the excited extra electron, the resulting σ-like molecular orbitals are destabilized relative to the π-like orbitals.

Figure 5 is a correlation diagram of the energy levels resulting from ligand and alkaline earth cation interactions. The BH_4^- ligand only partially lifts the p- and d-orbital degeneracy of the Ca^+ or Sr^+ atom. In addition, the BH_4^- ligand mixes the p and d character of the atomic orbitals so that the $\tilde{A}^2A_1$ state is a $p\sigma$–$d\sigma$ mixture while the $\tilde{B}^2E$ state is a $p\pi$–$d\pi$ mixture. The location of the ${}^2\Delta$ state is uncertain, but we suspect (contrary to Figure 5) that the ${}^2\Delta$ state lies above the $\tilde{A}$ and $\tilde{B}$ states for $CaBH_4$ and $SrBH_4$.

Conclusion

We have discovered the $CaBH_4$ and $SrBH_4$ molecules by the reaction of Ca and Sr vapors with diborane. The low-resolution spectra are consistent with a tridentate molecular structure of C_{3v} symmetry with three bridging hydrogens. No evidence of fluxional behavior has been found yet, but the possibility cannot be ruled out. Some ab initio calculations on the alkaline earth monoborohydrides would be most welcome.

Acknowledgment. This research was supported by the National Science Foundation (CHE-8608630, CHE-8913785) and the Astronautics Laboratory, Edwards Air Force Base, CA.

---

(30) Brazier, C. R.; Bernath, P. F. *J. Mol. Spectrosc.* **1985**, *114*, 163–173. Hilborn, R. C.; Zhu, Q.; Harris, D. O. *J. Mol. Spectrosc.* **1983**, *97*, 73–91. Nakagawa, J.; Wormsbecher, R. F.; Harris, D. O. *J. Mol. Spectrosc.* **1983**, *97*, 37–64.

Methyl Chloride/Formic Acid van der Waals Complex: A Model for Carbon as a Hydrogen Bond Donor

Charles H. Reynolds

Contribution from the Computer Applications Research Department, Rohm and Haas Company, Spring House, Pennsylvania 19477. Received September 22, 1989

Abstract: AM1 and MP2/6-31+G*//6-31G** + ZPE calculations are reported for the van der Waals complex of formic acid and methyl chloride. Both theoretical approaches predict the formation of a relatively strong C–H···O hydrogen bond. Four minima were located for the formic acid/methyl chloride van der Waals complex, with hydrogen bond strengths ranging from 2.12 to 5.03 kcal/mol. The strength of this interaction argues that carbon may act as a hydrogen bond donor more readily than is generally assumed. Additionally, the computed formic acid/methyl chloride hydrogen bond has significant implications for polymer compatibility by providing support for the hypothesis that compatibility of PVC/acrylate polymer blends is attributable to the formation of C–H···O hydrogen bonds.

Introduction

Interest in carbon as a hydrogen bond donor stems from the role this type of hydrogen bond is increasingly thought to play in diverse areas of chemistry.[1] The C–H···X hydrogen bond has been implicated as a factor in determining crystal-packing structures for a variety of molecules,[2,3] particularly biomolecules,[4,5] in the anaesthetic mode of action[6] for certain halogenated compounds such as chloroform; and in polymer miscibility.[7] The latter is a topic of special importance due to burgeoning commercial interest in polymer blends.

Carbon as a hydrogen bond donor has been the subject of three extensive surveys of the crystallographic literature,[3,8,9] all of which concluded that carbon can indeed act as a hydrogen bond donor under certain circumstances. Theoretical[10–16] and experimental[1,17] studies aimed at determining the magnitude of C–H···X hydrogen bonds are limited, but those that are available indicate interaction energies as large as −5.4 kcal/mol for systems such as malononitrile and water.[11] This certainly constitutes a respectable hydrogen

---

(1) Green, R. D. *Hydrogen Bonding by C-H Groups*; Wiley: New York, 1974.

(2) Sarma, J. A. R. P.; Desiraju, G. R. *Acc. Chem. Res.* **1986**, *19*, 222.

(3) Taylor, R.; Kennard, O. *Acc. Chem. Res.* **1984**, *17*, 320.

(4) Saenger, W. *Angew. Chem., Int. Ed. Engl.* **1973**, *12*, 591.

(5) Jeffrey, G. A.; Maluszynska, H. *Int. J. Biol. Macromol.* **1982**, *4*, 173.

(6) Sandorfy, C.; Buchet, R.; Lussier, L. S.; Menassa, P.; Wilson, L. *Pure Appl. Chem.* **1986**, *58*, 1115.

(7) Olabisi, O.; Robeson, L. M.; Shaw, M. T. *Polymer-Polymer Miscibility*; Academic Press: New York, 1979.

(8) Desiraju, G. R. *J. Chem. Soc., Chem. Commun.* **1989**, 179.

(9) Taylor, R.; Kennard, O. *J. Am. Chem. Soc.* **1982**, *104*, 5063.

(10) Deakyne, C. A. Ionic Hydrogen Bonds Part II. Theoretical Calculations. In *Molecular Structure and Energetics*; Liebman, J. F.; Greenberg, A., Eds.; VCH: New York, 1987; Vol. 4.

(11) Kumpf, R. A.; Damewood, J. R., Jr. *J. Chem. Soc., Chem. Commun.* **1988**, 621.

(12) Tamura, Y.; Yamamoto, G.; Oki, M. *Chem. Lett.* **1986**, 1619.

(13) Oi, T.; Sekreta, E.; Ishida, T. *J. Phys. Chem.* **1983**, *87*, 2323.

(14) Popowicz, A.; Ishida, T. *Chem. Phys. Lett.* **1981**, *83*, 520.

(15) Vishveshwara, S. *Chem. Phys. Lett.* **1978**, *59*, 26.

(16) Berkovitch-Yellin, Z.; Leiserowitz, L. *J. Am. Chem. Soc.* **1982**, *104*, 4052.

(17) Meot-Ner (Mautner), M. *Acc. Chem. Res.* **1984**, *17*, 186.

0002-7863/90/1512-7903$02.50/0 © 1990 American Chemical Society